Biology Faculty Publications

Biology Department

1-1-2023

# Enhancement of Developmental Defects in the Boron-Deficient Maize Mutant tassel-less1 by Reduced Auxin Levels

Michaela S. Matthes
*University of Missouri*

Norman B. Best
*University of Missouri*

Janlo M. Robil
*University of Missouri*

Paula McSteen
*University of Missouri*

Follow this and additional works at: https://archium.ateneo.edu/biology-faculty-pubs

Part of the Agriculture Commons, Genetics and Genomics Commons, and the Plant Sciences Commons

## Recommended Citation

Matthes, M. S., Best, N. B., Robil, J. M., & McSteen, P. (2023). Enhancement of developmental defects in the boron-deficient maize mutant tassel-less1 by reduced auxin levels. Journal of Plant Nutrition and Soil Science, 00, 1–10. https://doi.org/10.1002/jpln.202300155

**RESEARCH ARTICLE**

# Enhancement of developmental defects in the boron-deficient maize mutant *tassel-less1* by reduced auxin levels

**Michaela S. Matthes**[1,2] | **Norman B. Best**[1,3] | **Janlo M. Robil**[1,4] | **Paula McSteen**[1]

[1]Division of Biological Sciences, Bond Life Sciences Center, Interdisciplinary Plant Group and Missouri Maize Center, University of Missouri, Columbia, Missouri, USA

[2]Institute of Crop Science and Resource Conservation, Crop Functional Genomics, University of Bonn, Bonn, Germany

[3]USDA-ARS Plant Genetics Research Unit, Columbia, Missouri, USA

[4]Department of Biology, School of Science and Engineering, Ateneo de Manila University, Quezon, Manila, Philippines

**Correspondence**
Michaela S. Matthes, Rheinische Friedrich Wilhelms Universität Bonn, Institute of Crop Science and Resource Conservation, Crop Functional Genomics, Friedrich-Ebert-Allee 144, 53113 Bonn, Germany.
Email: mmatthes@uni-bonn.de

This article has been edited by Monika Wimmer.

**Abstract**

**Background:** Plant responses to deficiencies of the micronutrient boron are diverse and go beyond the well-characterized function of boron in cell wall crosslinking. To explain these phenotypic discrepancies, hypotheses about interactions of boron with various phytohormones have been proposed, particularly auxin. While these hypotheses are intensely tested in the root meristem of the model species, *Arabidopsis thaliana*, studies in crop species and the shoot are limited.

**Aims:** To address potential boron–auxin interactions during the vegetative and reproductive development of the crop maize (*Zea mays*), we utilized the boron-deficient *tassel-less1* (*tls1*) mutant and the auxin-deficient *vanishing tassel2* (*vt2*) mutant. We investigated interactions of boron and auxin on the levels of auxin biosynthesis and auxin transport in leaves and shoot meristems.

**Methods and Results:** By using genetic interaction analysis, hormone quantification, and confocal microscopy, we show that boron-deficient leaf phenotypes in *tls1* are enhanced in double mutants with *vt2* in both greenhouse and field conditions. However, auxin levels are not altered in developing leaves in *tls1*. Rather, the localization of *Zm*PIN1a:YFP, a marker for auxin transport, is altered in young tassel meristems and is absent from organ initiation sites during vegetative development.

**Conclusions:** Our data suggest a link between polar auxin transport and phenotypic consequences in boron-deficient conditions and further show that boron deficiency-induced developmental defects are sensitive to low auxin levels. Our study, therefore, offers new insight into nutrient–hormone interactions to regulate crop development.

**KEYWORDS**
auxin, boron, *Knotted1*, maize, *tassel-less1*, *vanishing tassel2*

## 1 | INTRODUCTION

Postembryonic plant development depends on the activity of plant stem cells, found in specific tissues called meristems. Since the discovery of the essentiality of boron (Warington, 1923), its role in meristem development was found to be critical. This is equally true for above- and below-ground meristems. The root reacts first to a lack of boron with inhibition of primary and lateral root growth (Warington, 1923). This inhibition is later also manifested in the shoot (Sommer & Sorokin, 1928). While the phenotypic defects appear to be correlated with boron's best-characterized role of crosslinking the pectic subunits Rhamnogalacturonan II in the primary cell wall (Kobayashi et al., 1996; Matoh, 1997; O'Neill et al., 1996), additional evidence for a role of boron in the plasma membrane (Voxeur & Fry, 2014; Wimmer

et al., 2009), interactions of boron with various phytohormones (Abreu et al., 2014; Camacho-Cristóbal et al., 2015; Eggert & von Wirén, 2017; Gómez-Soto et al., 2019; Martín-Rejano et al., 2011; Matthes et al., 2022; Matthes & Torres-Ruiz, 2016; Pommerrenig et al., 2022; Poza-Viejo et al., 2018; Wang et al., 2006), and potential involvement of boron in transcriptional responses have been reported (Camacho-Cristóbal et al., 2008; Peng et al., 2012). While these roles of boron correlate with boron deficiency-induced phenotypic defects, a functional or mechanistic link besides boron's cell wall function has not been shown thus far. Particularly, hypotheses about potential interactions of boron with the phytohormone auxin are longstanding, since it was already shown in 1940 that boron deficiency symptoms in *Gossypium herbaceum* (cotton) resembled auxin deficiency symptoms and that auxin could at least partially replace boron (Eaton, 1940). Nowadays, auxin is considered the main regulator of root elongation under boron deficiency in *Arabidopsis thaliana* (Arabidopsis) (as reviewed in Chen et al., 2023). In the crop *Zea mays* (maize), the functional involvement of auxin in the boron deficiency-induced phenotypic defects remains to be tested.

In maize, boron deficiency-induced defects are mainly studied in shoot meristems, since maize shoot meristems are particularly sensitive to low boron levels, as seen in the boron transporter mutants, *tassel-less1* (*tls1*) (Durbak et al., 2014; Leonard et al., 2014), *rotten ear* (*rte*) (Chatterjee et al., 2014), and *rte2* (Chatterjee et al., 2017). Additionally, the genetics of shoot meristem development in maize are well understood (as reviewed in Somssich et al., 2016). Phenotypes of the maize boron transporter mutants depend on soil boron concentrations, where defects in both male (tassel) and female (ear) reproductive structures are observed in adequate boron conditions (as reviewed in Matthes et al., 2020). In low boron conditions, boron transporter mutants also show vegetative phenotypes like short and narrow leaves, enhanced tillering, and in extreme cases seedling lethality (Durbak et al., 2014). Similar phenotypes are also observed in auxin biosynthesis and signaling mutants in maize (Barazesh & McSteen, 2008; Gallavotti, Barazesh, et al., 2008; Galli et al., 2015; Phillips et al., 2011), suggesting a functional role of the auxin pathway for boron-dependent development in maize. Here, we tested this hypothesis by investigating the involvement of auxin biosynthesis and auxin transport in affecting *tls1* shoot development. Our results indicate that under boron-deficient conditions, reduced auxin biosynthesis affects vegetative development more than reproductive development. In addition, defects in auxin transport were identified as early defects in boron-deficient *tls1* meristems, suggesting these might contribute to both the vegetative and reproductive phenotypes observed in the *tls1* mutant. Our results, therefore, indicate significant, tissue-specific interactions of boron and auxin in maize shoot meristems.

## 2 | MATERIALS AND METHODS

### 2.1 | Growing conditions

Greenhouse experiments were performed in the Sears Plant Growth Facility on the University of Missouri Campus, equipped with 1000-W HPS lamps. Plants were grown under long-day conditions (16 h of light and 8 h of dark) with an average day temperature of 30.5°C, an average night temperature of 25°C, and average humidity of 40% (day) and 60% (night). Plants were fertilized with Peters General Purpose 20−20−20 fertilizer (ICL specialty fertilizers) with every watering and the strength adjusted to 238 mg kg$^{-1}$ total nitrogen, which corresponds to a boron concentration of 0.08 mg kg$^{-1}$ (Matthes et al., 2018). Although not the most balanced fertilizer formulation for plant growth, no maize growth differences were reported for the 20:20:20 formulation compared to other fertilizer formulations (Kottkamp et al., 2010) and, in our hands, it controlled for nitrogen deficiency symptoms. The double mutant analysis was performed two times in the greenhouse with comparable results.

Field experiments were performed in Molokai, HI, during the winter season in 2017, 2018, and 2019, and at the Genetics Farm in Columbia, MO, during the summer season in 2017, 2018, and 2019. The double mutant analysis was performed three times with comparable results. Soil boron concentration in Missouri averages about 0.39 mg kg$^{-1}$, which is considered borderline boron-deficient and leads to severe vegetative defects in *tls1* including seedling lethality (Durbak et al., 2014; Matthes et al., 2018). The field site on Molokai, HI, has an average soil boron concentration of 1.19 mg kg$^{-1}$, which are adequate soil boron levels, indicated by less severe phenotypes in *tls1*, which grows to maturity in HI. Therefore, the HI field site allowed phenotypic analysis of mature tassels in *tls1* mutants. Soil boron levels were analyzed by the Soil and Plant Testing Laboratory at the University of Missouri, using hot water-soluble boron extraction methods followed by azomethine H for determination (Lohse, 1982).

### 2.2 | Plant material and phenotyping

The *tls1* segregating families were derived from the *tls1-ref* allele (Albertsen et al., 1993). The *tls1* families were backcrossed four times into the B73 inbred line, and individuals were genotyped by using the closely linked PCR marker idp8530 (Durbak et al., 2014). The *vanishing tassel2-ref* (*vt2*) allele originated from transposon mutagenesis (Smith & Hake, 1993) and was backcrossed into the B73 inbred line six times. The genotyping of *vt2* individuals was performed as previously published (Phillips et al., 2011). Since both mutants are sterile, *vt2* heterozygous plants were crossed with *tls1* heterozygous plants, and the resulting progeny was self-pollinated to obtain families segregating both single and double mutants. The *Zm*PIN1a:YFP translational fusion line was backcrossed into the B73 inbred line three times prior to crossing and backcrossing to *tls1* heterozygous plants. Wild-type siblings from segregating families were used as controls in all analyses. Despite careful introgression of the respective mutants and the transgene, the authors acknowledge that the effects of the mutation or transgene observed in the present study could also be due to linked mutations in the mutants and/or background introgression effects.

The development of a tassel (tassel formation) was scored as follows: 1 = full tassel and 0 = no tassel. Plant height measurements at maturity were taken from the pot soil (greenhouse) or soil (field) level

up to the tip of the tassel (total plant height) and the leaf collar of the flag leaf (plant height to flag leaf). The leaves from the seedling stage to the reproductive stage were marked in order to count the total leaf number. Leaf length was determined by measuring the total leaf blade length, and leaf width was determined by measuring the width of the leaf blade at the midpoint.

## 2.3 | Confocal microscopy

For confocal microscopy, developing tassel meristems (about 1 mm in size) of families segregating *tls1* harboring the *Zm*PIN1a:YFP construct (translational fusion) (Gallavotti, Yang, et al., 2008; Krishnakumar et al., 2015) were visualized with an inverted Leica SP8 confocal microscope (Leica) equipped with a tunable white light laser using 10× and 40× objectives (HCX PL APO CS 10×/0.40 dry and HC PL APO CS2 40×/1.10 water). *Zm*PIN1a:YFP fluorescence was imaged using 514 nm excitation and 525–600 nm emission. Two to five individual meristems per genotype were imaged per confocal experiment, and the confocal experiment was performed three times. YFP genotyping was done using YFP-FW: GAC CAC ATG AAG CAG CAC GAC and YFP-REV: GAG CTG CAC GCT GCC GTC primers.

Confocal image analysis was performed using ImageJ (Schneider et al., 2012). To obtain fluorescence intensities of the confocal images, the area and the integrated intensity of the respective meristem were measured. From that, the background intensity was subtracted to yield the corrected fluorescence intensities:

$$\text{Corrected fluorescence intensities} = \text{Integrated density}$$
$$- (\text{Area of selected cell} \times \text{Mean fluorescence of}$$
$$\text{background readings}). \tag{1}$$

## 2.4 | Hormone analysis

For hormone analysis, 0.5-cm sections of developing leaf tissue from the two youngest leaves in the whorl of V6–V7 stage maize plants were harvested from approximately 5 mm above the base of the developing tassel meristem (tassel meristem size between 0.8 and 1 mm). All leaf samples were immediately frozen in liquid nitrogen. Per replicate and genotype, between nine and 10 leaf samples were pooled and sent to the Proteomics and Metabolomics Facility at the University of Nebraska Center for Biotechnology for targeted quantification of different auxin species using liquid chromatography–mass spectrometry (LC–MS) approaches (for details of the analysis procedure, see Supporting Information Data set S1).

## 2.5 | Mining of *tls1* RNA-sequencing data set

We made use of the previously published *tls1* tassel meristem RNA-sequencing data set (Matthes et al., 2022), which is available at NCBI's

Gene Expression Omnibus with the accession number GSE169600 (https://www.ncbi.nlm.nih.gov/geo/query/acc.cgi?acc=GSE169600).

Targeted gene lists were created by using published auxin-related genes (Matthes et al., 2019), published *kn1* targets (Bolduc et al., 2012), and searching maizeGDB with the search term "gretchen hagen" to identify genes involved in auxin catabolism (Table S1).

## 2.6 | Statistical analysis

Phenotypic traits in the double mutant analysis were analyzed using analysis of variance in R using the *multcompview* (Piepho, 2004) and *agricolae* packages (de Mendiburu & Yaseen, 2020). The Tukey test was used for post hoc correction for multiple comparisons at a significance level of $p < 0.05$. All sample numbers are displayed in the respective figures and tables. Statistical significance between normal and *tls1-ref* corrected fluorescence intensities was analyzed using Student's *t*-test using the Microsoft Excel software (Student, 1908).

## 3 | RESULTS

Hypotheses about potential boron–auxin interactions go back to studies with cotton, where it was shown that auxin can replace boron in boron deficiency conditions (Eaton, 1940). In Arabidopsis, auxin is now considered the main regulator of root elongation under boron deficiency (as reviewed in Chen et al., 2023). In maize, boron–auxin interactions have previously not been investigated. In order to address such interactions in maize, we tested whether altered auxin biosynthesis affects the vegetative and reproductive phenotypes of the boron deficiency mutant *tls1* and whether auxin transport is altered in this mutant.

## 3.1 | The role of auxin in shoot development in boron-deficient conditions

### 3.1.1 | The *tls1*-induced leaf defects are enhanced by *vt2*

Phenotypes of the boron-deficient *tls1* mutant vary depending on the boron conditions the mutants are grown in. When boron levels are low, *tls1* mutants show severe vegetative defects with short and stiff leaves and seedling lethality, while in adequate or high boron conditions, *tls1* has pronounced reproductive defects (Durbak et al., 2014). In order to assess whether auxin levels are crucial for vegetative and reproductive development in boron-deficient conditions, we performed double mutant analyses between *tls1* and the auxin biosynthesis mutant *vt2* in the greenhouse. The *vt2* mutant produces only 34% of the active auxin indole-3-acetic acid (IAA) in developing leaves compared to the measured IAA levels in normal siblings (Phillips et al., 2011). In greenhouse experiments, the *tls1;vt2* double mutant plants
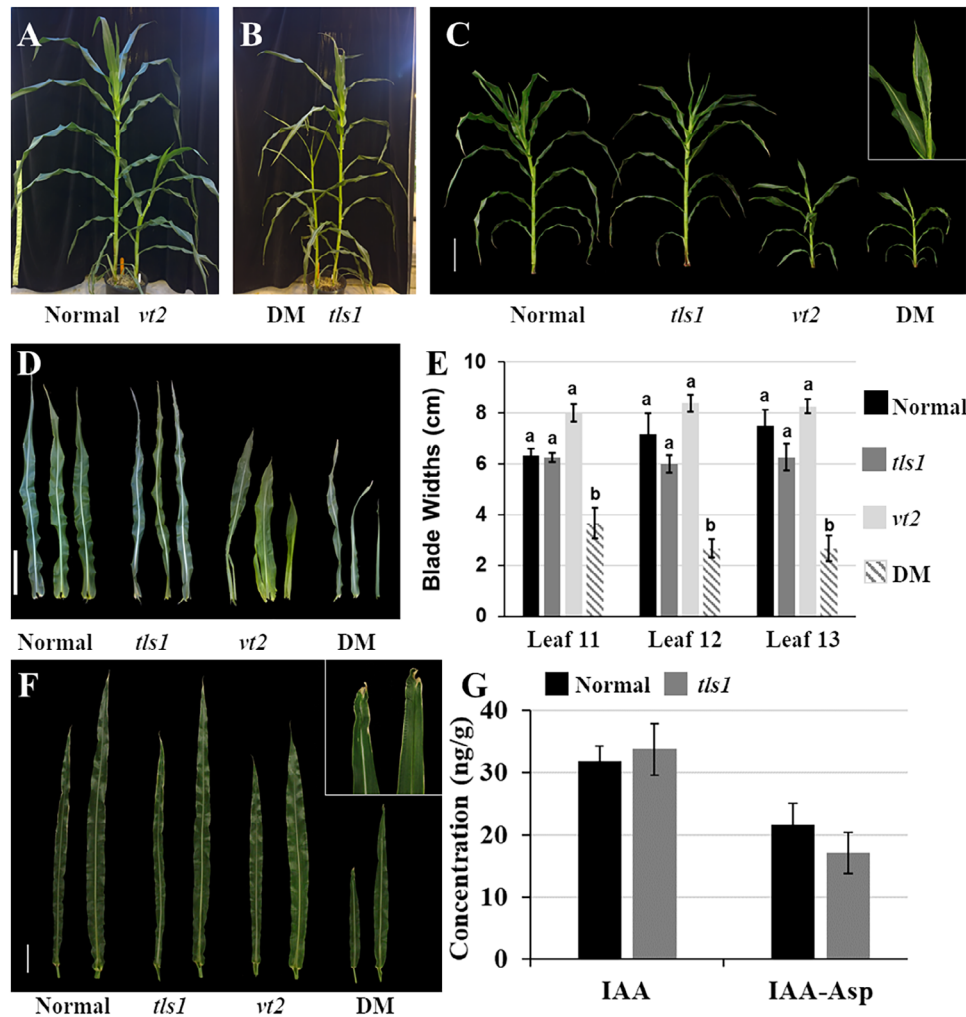
**FIGURE 1** Vegetative boron deficiency defects are sensitive to auxin levels. (A–C) Full plant phenotypes of (A) normal plant and *vt2* single mutant (Greenhouse 2019); (B) DM and *tls1* single mutant (Greenhouse 2019); (C) indicated genotypes (Greenhouse 2020); (D) leaf images of different genotypic categories of a *tls1;vt2* double mutant family grown in the greenhouse 2019. Depicted are leaves 11, 12, and 13 for each genotypic category. (E) Statistical analysis of leaf widths in the *tls1;vt2* double mutant family as shown in (D). (F) Leaf images of different genotypic categories of a *tls1;vt2* double mutant family grown in the greenhouse 2020. Depicted are leaves seven (left) and nine (right) of the respective genotypic categories. (G) Statistical analysis of levels of different auxin species in Normal and *tls1* leaves measured by LCMS (*n* = 3). Statistical analyses in (E) and (G) depict averages with standard error of means with a connecting letter report indicating statistical significance (*p* < 0.05) according to an analysis of variance with *post hoc* Tukey test (E) or according to Student's *t*-test (G). Sample sizes in (E) are Normal = 3, *tls1* = 2, *vt2* = 4, DM = 3. Scale bars in (C) = 20 cm, (D) and (F) = 10 cm. Pot size is the same in (A) and (B). IAA, Indole-3-acetic acid; Asp, aspartate; DM, *tls1;vt2* double mutant; LCMS, liquid chromatography-mass spectrometry; *tls1, tassel-less1*; *vt2, vanishing tassel2*.

developed into short plants with pronounced leaf defects (Figure 1), resembling *tls1* single mutants in boron-deficient conditions (Durbak et al., 2014; Matthes et al., 2022). This was surprising, since the *tls1* single mutants depicted only reproductive phenotypes in the greenhouse (Matthes et al., 2018) and suggested an enhancement of *tls1*-induced defects by the loss of *vt2*. In addition, leaf blade widths of leaves 11,12, and 13, which are closest to the tassel, were significantly narrower in *tls1;vt2* double mutants (developmental stage: V14) compared to either single mutant and the normal siblings (Figure 1; Table S2). Earlier in development (developmental stage: V12), leaf blade lengths of older *tls1;vt2* leaves (leaves 6, 7, 8) were significantly shorter compared to either single mutant (Table S3). These results showed that the *tls1*-induced leaf defects were enhanced by a loss of *vt2*. Plant height and

leaf number of *tls1;vt2* double mutants were not enhanced and resembled *vt2* (Tables S2 and S3). These results showed that the leaf growth defects of *tls1* were particularly enhanced in *tls1;vt2* double mutants, suggesting that the *tls1*-induced leaf defects are sensitive to auxin levels.

### 3.1.2 | Levels of IAA and IAA-aspartate are not altered in *tls1* leaves

If altered auxin levels were causative for the observed leaf defects in *tls1*, we hypothesized that auxin levels would be altered early during leaf development. We therefore analyzed levels of different auxin
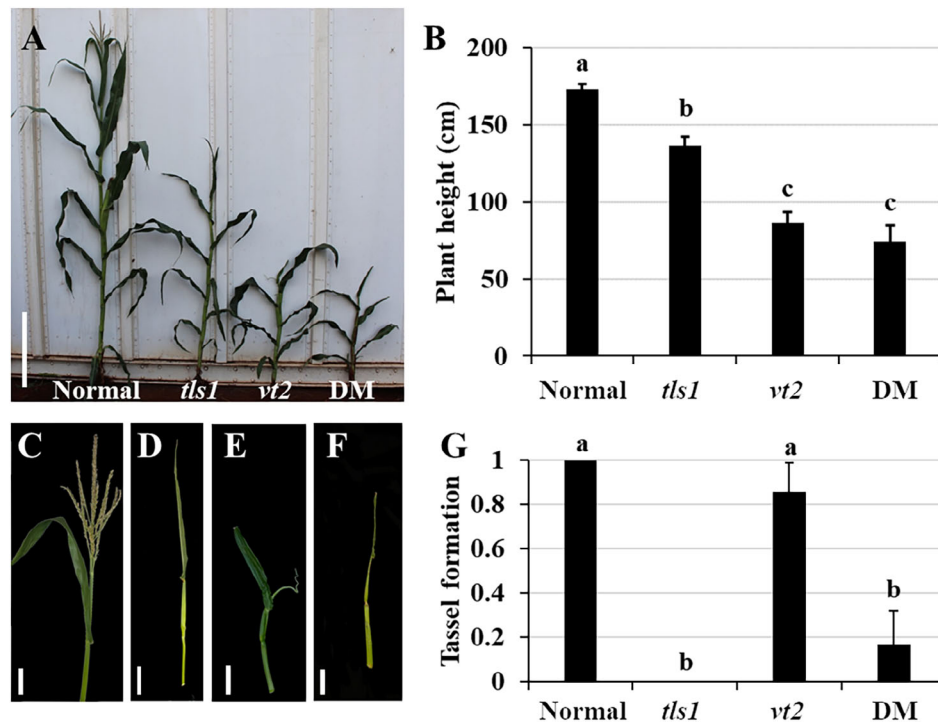
**FIGURE 2** Sensitivity of *tls1*-induced vegetative and reproductive defects to auxin levels in field conditions. (A) Plant pictures of different genotypic categories of a *tls1;vt2* double mutant segregating family grown in Hawaii in 2019. (B) Statistical analysis of total plant height in the *tls1;vt2* double mutant family as shown in (A). Tassel pictures of (C) Normal, (D) *tls1*, (E) *vt2*, and (F) *tls1;vt2* from a *tls1;vt2* double mutant segregating family. (G) Statistical analysis of tassel formation in the *tls1;vt2* double mutant family as shown in (C–F). The statistical analyses in (B) and (G) depict averages with standard error of means with a connecting letter report indicating statistical significance ($p < 0.05$) according to an analysis of variance with post hoc Tukey test. Sample sizes are Normal = 12, *tls1* = 12, *vt2* = 7, DM = 6. Scale bars in (A) = 20 cm and (C–F) = 5 cm. DM, *tls1;vt2* double mutant; *tls1, tassel-less1*; *vt2, vanishing tassel2*.

species using LC–MS analysis from developing leaves of *tls1* and normal siblings (Figure 1G). Our analysis showed unaltered levels of IAA and the auxin conjugate IAA-aspartate (Asp) in *tls1* mutants (Figure 1G). The auxin conjugates methyl-IAA and IAA-Tryptophan (Trp) were not detected in any sample analyzed. These results showed that *tls1* exhibits normal levels of auxin in developing leaves, suggesting that auxin biosynthesis is not affected during early leaf development in boron-deficient conditions.

### 3.1.3 | The role of auxin biosynthesis in *tls1* reproductive development

In addition to the greenhouse experiments, we analyzed the *tls1;vt2* double mutants also in field conditions with adequate boron concentration (Hawaii field site: soil boron concentration 1.19 mg/kg) (Figure 2). The plants were grown up to maturity, which allowed an investigation of reproductive phenotypes in the tassel in addition to vegetative defects. Similar to what we had observed in the greenhouse, the *tls1;vt2* double mutants had short, narrow leaves resembling *tls1* in low boron conditions (Figure 2A), indicating the enhancement of *tls1*-induced leaf defects by a loss of *vt2* also in field conditions. The *tls1* single mutants were shorter than normal siblings in field conditions (Figure 2B). While both *vt2* single mutants and the *tls1;vt2* double mutants were signif-

icantly shorter than both *tls1* single mutants and normal siblings, no statistical difference was detected between *vt2* and *tls1;vt2* double mutants (Figure 2B). Regarding tassel development, normal siblings always developed a tassel, while *tls1* single mutants segregating in *tls1;vt2* F2-families never developed a tassel (Figure 2C–G). While *vt2* single mutants mostly developed a tassel (86 ± 13%), *tls1;vt2* double mutants were not significantly different from *tls1* single mutants regarding tassel formation and mostly failed to develop a tassel (16.67 ± 15%). While the severe tassel phenotype in *tls1* hindered an analysis of potential defect enhancements by *vt2*, the analysis showed that reducing auxin biosynthesis does not suppress the *tls1*-induced tassel phenotype. Interestingly, flag leaf width and length in the *tls1;vt2* double mutants morphologically appeared severely reduced compared to *tls1* and *vt2* single mutants (compare Figure 2F with Figure 2D,E), again suggesting an enhancement of the *tls1*-induced leaf defects by *vt2* also in field conditions.

### 3.2 | *Zm*PIN1a localization and abundance are altered in *tls1* vegetative and reproductive meristems

Since the biological activity of auxin depends on not only its biosynthesis but also various other mechanisms, including its cell-to-cell, polar transport, we analyzed the localization of the auxin transport marker

line ZmPIN1a:YFP (Gallavotti, Barazesh, et al., 2008; Krishnakumar et al., 2015) in tls1 and normal sibling shoot meristems (Figure 3). In the normal vegetative shoot apical meristems (SAM), ZmPIN1a:YFP accumulated in organ primordia and appeared to be localized at the plasma membrane throughout the meristems (Figure 3A–C). In contrast, the localization and protein abundance of ZmPIN1a:YFP appeared weaker in tls1 vegetative SAMs (Figure 3D–F). Statistical analysis of corrected total fluorescence intensity showed that ZmPIN1a:YFP fluorescence was significantly reduced in tls1 SAMs compared to normal SAMs (Figure 3M), supporting a reduction of ZmPIN1a:YFP levels in the tls1 SAM compared to normal siblings. In addition, the accumulation of ZmPIN1a:YFP at organ initiation sites appeared to be missing/reduced in tls1 SAM (compare Figure 3B,C with Figure 3E,F), suggesting an altered ZmPIN1a:YFP distribution in tls1 SAMs. During tassel development, the accumulation of ZmPIN1a:YFP in the inflorescence meristem (IM) appeared similar between tls1 mutants and normal siblings, supported by statistical analysis of corrected total fluorescence intensity showing no statistical difference between normal and tls1 mutants (Figure 3M). In contrast, the accumulation of ZmPIN1a:YFP at the sites of bract/axillary meristem initiation (note arrows in Figure 3I,L) appeared weaker, and polar localization of ZmPIN1a:YFP in the IM of tls1 seemed more diffuse compared to normal siblings (compare Figure 3I with Figure 3L). Since no morphological differences could be observed in the analyzed SAM and IM stages, our results indicate that alterations of ZmPIN1a accumulation, distribution, and localization are early molecular defects in developing meristems under boron-deficient conditions. These results suggest that altered auxin transport contributes to the observed boron-deficiency-induced defects in the tls1 vegetative and tassel meristems, such as the reduction in SAM/IM size and reduced number of axillary meristems (Durbak et al., 2014). Older tassel meristems of tls1, which showed obvious morphological defects, had an enhancement of ZmPIN1a:YFP signal throughout the IM (Figure S1).

## 3.3 | Specific auxin-related genes are differentially expressed in tls1 developing tassel meristems

We have previously reported a transcriptomics analysis in developing tassel meristems of tls1. In this experiment, tls1 meristems were morphologically similar to meristems of normal siblings, enabling the detection of early molecular responses in boron-deficient conditions. This analysis showed that defects in tls1 are specific and correlate with an early downregulation of the meristem maintenance gene knotted1 (kn1) (Matthes et al., 2022). To further understand, how auxin-related pathways might contribute to the observed tassel defects in tls1, we mined the tls1 tassel meristem RNA-sequencing data set for auxin-related genes (Table S1). Out of the 283 auxin-related genes from our search list, we detected 10 to be significantly differentially expressed in developing tls1 tassel meristems (Table 1). There were four auxin amido synthetases (auxin conjugation), three AUXIN(AUX)/INDOLE-3-ACETICACID (IAA) genes (auxin signaling), one ABCB/PGP (auxin transport), one AUXIN RESPONSE FACTOR (ARF) gene (auxin signaling),

and one auxin response gene. The detected auxin amido synthetases, the AUX/IAA genes, and the auxin response gene were significantly upregulated in tls1, while the ARF gene (arf35, clade A = transcriptional activator) and the ABCB/PGP gene were significantly downregulated (Table 1). These results suggested that auxin homeostasis, transport, and signaling may be altered in young tls1 tassel meristems. Interestingly, out of the 10 detected auxin-related genes, six were also reported to be KN1 targets in meristems (Table 1) (Bolduc et al., 2012), supporting the possibility that an interaction between boron and auxin during meristem development is mediated through KN1 function.

# 4 | DISCUSSIONS

Potential boron–auxin interactions are longstanding (Eaton, 1940). While auxin appears to be the main regulator of boron-deficiency-induced root elongation defects in Arabidopsis (as reviewed in Chen et al., 2023), involvement of auxin in the developmental defects of the maize shoot in boron-deficient conditions is not known. We therefore tested whether auxin biosynthesis affects the vegetative and reproductive phenotypes of the boron-deficient tls1 mutant and whether ZmPIN1a:YFP patterns are altered in tls1.

## 4.1 | Boron deficiency-induced leaf defects are sensitive to low auxin levels

The biological activity of auxin is evoked through free IAA, and its local concentration can be affected by various mechanisms, including auxin biosynthesis, transport, synthesis of IAA conjugates, and catabolism. While altered auxin levels have been observed in boron-deficient conditions in various species, a mechanistic understanding of such observations is missing. It has been postulated that boron might control effective auxin concentrations through the enhancement of auxin oxidases (Blevins & Lukaszewski, 1998; Jarvis et al., 1983) and that boron levels affect the expression of auxin biosynthesis genes, for example, in trifoliate oranges (Q. Li et al., 2016). In maize, mining a tls1 tassel transcriptome data set revealed that several auxin amido synthetases, involved in the conjugation of IAA, were differentially regulated, but no auxin biosynthesis genes were detected (Table 1). Although boron deficiency-induced leaf defects were enhanced in double mutants of tls1 with the auxin biosynthesis mutant vt2, in both greenhouse and field conditions (Figures 1 and 2; Tables S2 and S3), auxin levels were not altered in young developing leaves of tls1 (Figure 1G). The significantly narrower leaf blades in tls1;vt2 double mutants suggest a suppression of the broad leaf phenotype in vt2 which is due to an increased medial-lateral growth during early leaf development (Robil et al., 2021; Robil & McSteen, 2023). These findings show that leaf expansion defects in tls1 are sensitive to auxin levels and that potential auxin level defects responsible for the observed leaf expansion defects in tls1 are likely not mediated by altered auxin biosynthesis.
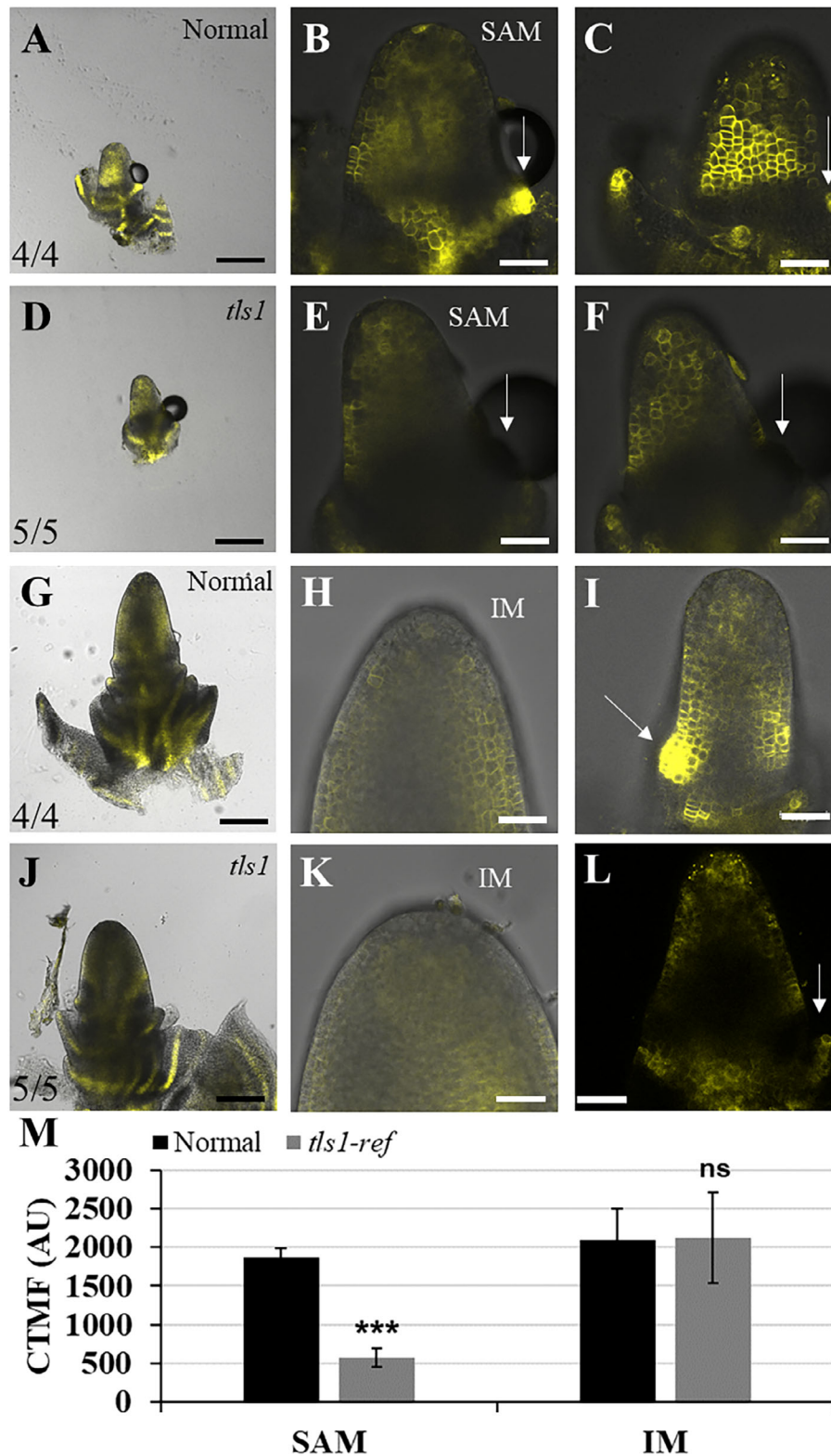
**FIGURE 3** *Zm*PIN1a:YFP localization and abundance are altered in *tls1* meristems. Confocal microscopy of *Zm*PIN1a:YFP in (A–C) Normal vegetative meristems; (D–F) *tls1* vegetative meristems; (G–I) normal tassel meristems. (J–L), *tls1* tassel meristems. (M) Statistical analysis of corrected total meristem fluorescence intensities in shoot apical and inflorescence meristems of *tls1* and normal siblings. Depicted are means with standard error of means ($n = 4$ [normal] and $n = 5$ [*tls1*]). Statistical significance was calculated using Student's *t*-test, where ***$p < 0.005$. Scale bars in (A), (D), (G), and (J) = 200 µm; (B), (C), (E), (F), (H), (I), (K), and (L) = 50 µm. Arrows in (B), (C), (E), (F), (I), and (L) point to the presence (B, C, and I) or absence (E, F, and L) of *Zm*PIN1a:YFP accumulation in organ primordia/axillary meristems using the same confocal settings. Numbers in A, B, G, and J indicate how often the respective pattern was observed. AU, arbitrary units; CTMF, corrected total meristem fluorescence intensity; IM, inflorescence meristem; ns, not statistically significantly different; SAM, shoot apical meristem; *tls1*, *tassel-less1*.

**TABLE 1** Significantly differentially regulated genes in *tassel-less1* (*tls1*) developing tassel meristems.

| GeneIdentifier_v4 | GRMZM-Number | $\log_2$FC | padj | KNBOUND | AuxinAll |
|---|---|---|---|---|---|
| Zm00001d014690 | GRMZM2G317900 | −0.51 | 0.000465775 | KNBOUND | ARF35 |
| Zm00001d029577 | GRMZM2G068701 | 1.03 | 0.001914179 | NV[a] | aas1 |
| Zm00001d010697 | GRMZM2G366873 | 1.65 | 4.04363E-06 | NV[a] | aas12 |
| Zm00001d006753 | GRMZM2G378106 | 1.39 | 0.000295417 | KNBOUND | aas2 |
| Zm00001d022017 | GRMZM2G053338 | 1.11 | 0.005072481 | KNBOUND | aas8 |
| Zm00001d018414 | GRMZM2G030465 | 1.4 | 9.22106E-06 | KNBOUND | IAA17 |
| Zm00001d021279 | GRMZM2G149449 | 1.45 | 0.000697212 | NV[a] | IAA26/IAA24 |
| Zm00001d041416 | GRMZM2G138268 | 0.75 | 0.001084134 | KNBOUND | IAA7 |
| Zm00001d052618 | GRMZM2G159854 | 0.37 | 0.009009365 | NV[a] | Protein AUXIN RESPONSE 4 |
| Zm00001d045269 | GRMZM2G111903 | −0.72 | 0.006430756 | KNBOUND | ZmABCB/PGP |

*Note*: KNBOUND = respective gene was found to be a target of the transcription factor and meristem maintenance regulator KNOTTED1 (Bolduc et al., 2012).

Abbreviations: FC, Fold Change; aas, auxin amido synthetase.

[a]Not a target of KN1.

## 4.2 | Disturbances of *Zm*PIN1a as an early cellular response in *tls1* tassel meristems

In addition to auxin biosynthesis, the cell-to-cell, polar transport of auxin also mediates the levels of auxin. Boron deficiency was reported to reduce auxin export in *Pisum sativum* (C. Li et al., 2001; Wang et al., 2006) and was shown to alter the abundance and localization of the efflux transporter PIN1 in the Arabidopsis root meristem (K. Li et al., 2015) and embryo (Matthes & Torres-Ruiz, 2016). In addition, expression levels of various auxin transporter genes were reduced in boron-deficient Arabidopsis roots (Camacho-Cristóbal et al., 2015). Our results showed alterations of *Zm*PIN1a:YFP in shoot apical and developing tassel meristems of *tls1*, particularly at organ initiation sites (Figure 3), suggesting altered auxin transport in *tls1*. It is tempting to speculate that altered distribution, accumulation, and localization of *Zm*PIN1a are early molecular phenotypes of boron limitation in maize, and it remains to be tested whether this is a direct or indirect defect mediated by boron deficiency-induced cell wall defects. Since polar auxin transport is important for mediating auxin maxima needed for lateral organ development (as reviewed, for example, in Taylor-Teeples et al., 2016), it can be speculated that early disturbances of the localization of *Zm*PIN1a in maize meristems would lead to altered auxin distribution patterns and therefore might locally lead to tissue-specific auxin deficiencies in boron deficient conditions. This in turn may lead to the observed leaf growth defects observed in *tls1* in severe boron-deficient conditions.

## 4.3 | Regulation of auxin-related genes through KN1 during tassel development in *tls1*

We recently proposed that a boron-dependent downregulation of the master meristem maintenance regulator gene, *kn1*, could be causative for the observed meristem maintenance defects in the *tls1* tassel

meristem (Matthes et al., 2022). An enrichment of KN1 targets was observed among the differentially expressed genes in the *tls1* tassel RNA-sequencing data set. Likewise, out of the 10 auxin-related genes that we detected to be differentially expressed in *tls1* tassel meristems compared to normal siblings, six were reported KN1 targets in meristems (Table 1) (Bolduc et al., 2012). Similarly, although not detected in the *tls1* data set, several auxin-related genes including *vt2* and various *PIN* genes are also direct targets of KN1 (Bolduc et al., 2012). Vegetative defects of *tls1* were enhanced in *tls1;vt2* (Figures 1 and 2; Tables S2 and S3), phenotypically similar to the recently reported phenotype of double mutants of *tls1* with *kn1* (Matthes et al., 2022). Our data, therefore, suggest that an alteration of *kn1* transcripts might also contribute to the observed sensitivity of boron-deficiency-induced leaf defects to auxin levels and add further evidence for an integral role of the transcription factor KN1 during meristem development in boron-deficient conditions.

## 5 | CONCLUSIONS

In this study, we show that the leaf defects of the boron deficiency maize mutant *tls1* are sensitive to auxin levels and that the localization of the auxin transporter *Zm*PIN1a is altered in the shoot apical and young tassel meristems of *tls1*. Our data therefore suggest tissue-specific interactions of boron and auxin, particularly at the level of auxin transport in the maize shoot. Our study highlights boron hormone interactions in the maize shoot, complementing recent findings of a central involvement of the meristem maintenance regulator KN1 in meristem development under boron-deficient conditions.

## DATA AVAILABILITY STATEMENT

The RNA-seq data set mentioned in this study is available at NCBI's Gene Expression Omnibus with the accession number GSE169600 (https://www.ncbi.nlm.nih.gov/geo/query/acc.cgi?acc=GSE169600). All other material is available from the corresponding author upon reasonable request.

## ORCID

*Michaela S. Matthes* https://orcid.org/0000-0001-5477-5846
*Norman B. Best* https://orcid.org/0000-0002-6572-5999
*Janlo M. Robil* https://orcid.org/0000-0002-0589-4766
*Paula McSteen* https://orcid.org/0000-0001-5319-5751

## REFERENCES

Abreu, I., Poza, L., Bonilla, I., & Bolaños, L. (2014). Boron deficiency results in early repression of a cytokinin receptor gene and abnormal cell differentiation in the apical root meristem of *Arabidopsis thaliana*. *Plant Physiology and Biochemistry*, 77, 117–121.

Albertsen, M. C., Trimnell, M. R., & Fox, T. (1993). Description and mapping of the *tassel-less1* (tls1) mutation. *Maize Newsletter*, 67, 51–52.

Barazesh, S., & McSteen, P. (2008). *Barren inflorescence1* functions in organogenesis during vegetative and inflorescence development in maize. *Genetics*, 179(1), 389–401.

Blevins, D. G., & Lukaszewski, K. M. (1998). Boron in plant structure and function. *Annual Review of Plant Biology*, 49(1), 481–500.

Bolduc, N., Yilmaz, A., Mejia-Guerra, M. K., Morohashi, K., O'Connor, D., Grotewold, E., & Hake, S. (2012). Unraveling the KNOTTED1 regulatory network in maize meristems. *Genes & Development*, 26(15), 1685–1690.

Camacho-Cristóbal, J. J., Herrera-Rodríguez, M. B., Beato, V. M., Rexach, J., Navarro-Gochicoa, M. T., Maldonado, J. M., & González-Fontes, A. (2008). The expression of several cell wall-related genes in Arabidopsis roots is down-regulated under boron deficiency. *Environmental and Experimental Botany*, 63(1–3), 351–358.

Camacho-Cristóbal, J. J., Martín-Rejano, E. M., Herrera-Rodríguez, M. B., Navarro-Gochicoa, M. T., Rexach, J., & González-Fontes, A. (2015). Boron deficiency inhibits root cell elongation via an ethylene/auxin/ROS-dependent pathway in Arabidopsis seedlings. *Journal of Experimental Botany*, 66(13), 3831–3840.

Chatterjee, M., Liu, Q., Menello, C., Galli, M., & Gallavotti, A. (2017). The combined action of duplicated boron transporters is required for maize growth in boron-deficient conditions. *Genetics*, 206(4), 2041–2051.

Chatterjee, M., Tabi, Z., Galli, M., Malcomber, S., Buck, A., Muszynski, M., & Gallavotti, A. (2014). The boron efflux transporter ROTTEN EAR is required for maize inflorescence development and fertility. *The Plant Cell*, 26(7), 2962–2977.

Chen, X., Smith, S. M., Shabala, S., & Yu, M. (2023). Phytohormones in plant responses to boron deficiency and toxicity. *Journal of Experimental Botany*, 74(3), 743–754.

de Mendiburu, F., & Yaseen, M. (2020). *Agricolae: Statistical procedures for agricultural research (version 1.4. 0).* https://github.com/myaseen208/agricolae

Durbak, A. R., Phillips, K. A., Pike, S., O'Neill, M. A., Mares, J., Gallavotti, A., Malcomber, S. T., Gassmann, W., & McSteen, P. (2014). Transport of boron by the *tassel-less1* aquaporin is critical for vegetative and reproductive development in maize. *The Plant Cell*, 26(7), 2978–2995.

Eaton, F. M. (1940). Interrelations in the effects of boron and indoleacetic acid on plant growth. *Botanical Gazette*, 101(3), 700–705.

Eggert, K., & von Wirén, N. (2017). Response of the plant hormone network to boron deficiency. *New Phytologist*, 216(3), 868–881.

Gallavotti, A., Barazesh, S., Malcomber, S., Hall, D., Jackson, D., Schmidt, R. J., & McSteen, P. (2008). *sparse inflorescence1* encodes a monocot-specific YUCCA-like gene required for vegetative and reproductive development in maize. *Proceedings of the National Academy of Sciences of the United States of America*, 105(39), 15196–15201.

Gallavotti, A., Yang, Y., Schmidt, R. J., & Jackson, D. (2008). The relationship between auxin transport and maize branching. *Plant Physiology*, 147(4), 1913–1923.

Galli, M., Liu, Q., Moss, B. L., Malcomber, S., Li, W., Gaines, C., Federici, S., Roshkovan, J., Meeley, R., Nemhauser, J. L., & Gallavotti, A. (2015). Auxin signaling modules regulate maize inflorescence architecture. *Proceedings of the National Academy of Sciences of the United States of America*, 112(43), 13372–13377.

Gómez-Soto, D., Galván, S., Rosales, E., Bienert, P., Abreu, I., Bonilla, I., & Bolaños, L. (2019). Insights into the role of phytohormones regulating pAtNIP5;1 activity and boron transport in *Arabidopsis thaliana*. *Plant Science*, 287, 110198. https://doi.org/10.1016/j.plantsci.2019.110198

Jarvis, B. C., Ali, A. H. N., & Shaheed, A. I. (1983). Auxin and boron in relation to the rooting response and ageing of mung bean cuttings. *New Phytologist*, 95(4), 509–518.

Kobayashi, M., Matoh, T., & Azuma, J. (1996). Two chains of rhamnogalacturonan II are cross-linked by borate-diol ester bonds in higher plant cell walls. *Plant Physiology*, 110(3), 1017–1020.

Kottkamp, J., Varjabedian, A., Ross, J., Eddy, R., & Hahn, D. T. (2010). *Optimizing greenhouse corn production: What is the best fertilizer formulation and strength?* Purdue Methods for Corn Growth. http://docs.lib.purdue.edu/pmcg/14

Krishnakumar, V., Choi, Y., Beck, E., Wu, Q., Luo, A., Sylvester, A., Jackson, D., & Chan, A. P. (2015). A maize database resource that captures tissue-specific and subcellular-localized gene expression, via fluorescent tags and confocal imaging (Maize Cell Genomics Database). *Plant and Cell Physiology*, 56(1), 1–7. https://doi.org/10.1093/pcp/pcu178

Leonard, A., Holloway, B., Guo, M., Rupe, M., Yu, G., Beatty, M., Zastro-Hays, G., Meeley, R., Llaca, V., Butler, K., Stefani, T., Jaqueth, J., & Li, B. (2014). *tassel-less1* encodes a boron channel protein required for inflorescence development in maize. *Plant and Cell Physiology*, 55(6), 1044–1054.

Li, C., Pfeffer, H., Dannel, F., Römheld, V., & Bangerth, F. (2001). Effects of boron starvation on boron compartmentation, and possibly hormone-mediated elongation growth and apical dominance of pea (*Pisum sativum*) plants. *Physiologia Plantarum*, 111(2), 212–219.

Li, K., Kamiya, T., & Fujiwara, T. (2015). Differential roles of PIN1 and PIN2 in root meristem maintenance under low-B conditions in *Arabidopsis thaliana*. *Plant and Cell Physiology*, *56*(6), 1205–1214.

Li, Q., Liu, Y., Pan, Z., Xie, S., & Peng, S. A. (2016). Boron deficiency alters root growth and development and interacts with auxin metabolism by influencing the expression of auxin synthesis and transport genes. *Biotechnology and Biotechnological Equipment*, *30*(4), 661–668.

Lohse, G. (1982). Microanalytical azomethine-H method for boron determination in plant tissue. *Communications in Soil Science and Plant Analysis*, *13*(2), 127–134.

Martín-Rejano, E. M., Camacho-Cristóbal, J. J., Herrera-Rodríguez, M. B., Rexach, J., Navarro-Gochicoa, M. T., & González-Fontes, A. (2011). Auxin and ethylene are involved in the responses of root system architecture to low boron supply in Arabidopsis seedlings. *Physiologia Plantarum*, *142*(2), 170–178.

Matoh, T. (1997). Boron in plant cell walls. *Plant and Soil*, *193*, 59–70.

Matthes, M. S., Best, N. B., Robil, J. M., Malcomber, S., Gallavotti, A., & McSteen, P. (2019). Auxin EvoDevo: Conservation and diversification of genes regulating auxin biosynthesis, transport, and signaling. *Molecular Plant*, *12*(3), 298–320.

Matthes, M. S., Darnell, Z., Best, N. B., Guthrie, K., Robil, J. M., Amstutz, J., Durbak, A., & McSteen, P. (2022). Defects in meristem maintenance, cell division, and cytokinin signaling are early responses in the boron deficient maize mutant *tassel-less1*. *Physiologia Plantarum*, *174*(2), e13670. https://doi.org/10.1111/ppl.13670

Matthes, M. S., Robil, J. M., & Mcsteen, P. (2020). From element to development: The power of the essential micronutrient boron to shape morphological processes in plants. *Journal of Experimental Botany*, *71*(5), 1681–1693.

Matthes, M. S., Robil, J. M., Tran, T., Kimble, A., & Mcsteen, P. (2018). Increased transpiration is correlated with reduced boron deficiency symptoms in the maize *tassel-less1* mutant. *Physiologia Plantarum*, *163*, 344–355.

Matthes, M., & Torres-Ruiz, R. A. (2016). Boronic acid treatment phenocopies *monopteros* by affecting PIN1 membrane stability and polar auxin transport in *Arabidopsis thaliana* embryos. *Development*, *143*(21), 4053–4062.

O'Neill, M. A., Warrenfeltz, D., Kates, K., Pellerin, P., Doco, T., Darvill, A. G., Albersheim, P., De, P., & Viala, P. (1996). Rhamnogalacturonan-II, a pectic polysaccharide in the walls of growing plant cell, forms a dimer that is covalently cross-linked by a borate ester. *The Journal of Biological Chemistry*, *271*(37), 22923–22930.

Peng, L., Zeng, C., Shi, L., Cai, H., & Xu, F. (2012). Transcriptional profiling reveals adaptive responses to boron deficiency stress in Arabidopsis. *Zeitschrift für Naturforschung C*, *67*(9–10), 510–524.

Phillips, K. A., Skirpan, A. L., Liu, X., Christensen, A., Slewinski, T. L., Hudson, C., Barazesh, S., Cohen, J. D., Malcomber, S., & McSteen, P. (2011). *vanishing tassel2* encodes a grass-specific tryptophan aminotransferase required for vegetative and reproductive development in maize. *Plant Cell*, *23*(2), 550–566.

Piepho, H. P. (2004). An algorithm for a letter-based representation of all-pairwise comparisons. *Journal of Computational and Graphical Statistics*, *13*(2), 456–466.

Pommerrenig, B., Faber, M., Hajirezaei, M.-R., von Wirén, N., & Bienert, G. P. (2022). Cytokinins as boron deficiency signals to sustain shoot development in boron-efficient oilseed rape. *Physiologia Plantarum*, *174*(5), e13776. https://doi.org/10.1111/ppl.13776

Poza-Viejo, L., Abreu, I., González-García, M. P., Allauca, P., Bonilla, I., Bolaños, L., & Reguera, M. (2018). Boron deficiency inhibits root growth by controlling meristem activity under cytokinin regulation. *Plant Science*, *270*, 176–189.

Robil, J. M., Gao, K., Neighbors, C. M., Boeding, M., Carland, F. M., Bunyak, F., & McSteen, P. (2021). grasviq: An image analysis framework for automatically quantifying vein number and morphology in grass leaves. *The Plant Journal*, *107*(2), 629–648.

Robil, J. M., & McSteen, P. (2023). Hormonal control of medial–lateral growth and vein formation in the maize leaf. *New Phytologist*, *238*(1), 125–141.

Schneider, C. A., Rasband, W. S., & Eliceiri, K. W. (2012). NIH Image to ImageJ: 25 Years of image analysis. *Nature Methods*, *9*(7), 671–675.

Smith, L. G., & Hake, S. (1993). A new mutation affecting tassel and ear morphology. *Maize Newsletter*, *67*, 2–3.

Sommer, A. L., & Sorokin, H. (1928). Effects of the absence of boron and of some other essential elements on the cell and tissue structure of the root tips of *Pisum sativum*. *Plant Physiology*, *3*(3), 237–260.

Somssich, M., Je, B. I., Simon, R., & Jackson, D. (2016). CLAVATA-WUSCHEL signaling in the shoot meristem. *Development*, *143*(18), 3238–3248.

Student (1908). The probable error of a mean. *Biometrika*, *6*(1), 1–25.

Taylor-Teeples, M., Lanctot, A., & Nemhauser, J. L. (2016). As above, so below: Auxin's role in lateral organ development. *Developmental Biology*, *419*(1), 156–164.

Voxeur, A., & Fry, S. C. (2014). Glycosylinositol phosphorylceramides from Rosa cell cultures are boron-bridged in the plasma membrane and form complexes with rhamnogalacturonan II. *The Plant Journal*, *79*(1), 139–149.

Wang, G., Römheld, V., Li, C., & Bangerth, F. (2006). Involvement of auxin and CKs in boron deficiency induced changes in apical dominance of pea plants (*Pisum sativum* L.). *Journal of Plant Physiology*, *163*(6), 591–600.

Warington, K. (1923). The effect of boric acid and borax on the broad bean and certain other plants. *Annals of Botany*, *37*(148), 629–672.

Wimmer, M. A., Lochnit, G., Bassil, E., Mühling, K. H., & Goldbach, H. E. (2009). Membrane-associated, boron-interacting proteins isolated by boronate affinity chromatography. *Plant and Cell Physiology*, *50*(7), 1292–1304.

## SUPPORTING INFORMATION

Additional supporting information can be found online in the Supporting Information section at the end of this article.